Spectroscopic Analysis of Combustion Process in CR DI Diesel Engine Operating in HCCI mode

E. Mancaruso, S. S. Merola, B. M. Vaglieco

Istituto Motori - C.N.R., Naples – ITALY

1. Introduction

In order to improve the engine performance, especially in terms of pollutant emissions, it seems feasible to combine homogeneous engine operation in the lower load range with conventional diesel engine operation at mid and high load. For this reason the Common Rail injection system is an important tool to create optimum mixture formation conditions for both homogeneous and conventional diesel combustion. A new combustion process was investigated in a Common Rail (CR) Direct Injection (DI) diesel engine. The process is named Homogeneous Charge Compression Ignition (HCCI) and it consists of ignition of homogeneous charge during the compression stroke of the engine. In HCCI mode, the fuel was injected far from the top death centre in order to produce a sufficient air/fuel (A/F) homogenisation. The homogeneity of the mixture solves the problem of rich mixture zones typical for diesel diffusion combustion. Moreover, local combustion temperature peaks, as they occur in the reaction zones of conventional diesel engines, are avoided. Combustion takes place with virtually no NO_x emission if the combustion temperature does not exceed the NO_x formation level [1-3].

In the present paper, HCCI combustion was applied to an optically accessible diesel engine equipped with high pressure multiple injections CR injection system. The use of very early injection timings has been proposed to meet the requirement of sufficient time for mixing of fuel and air. Combined measurements, based on digital imaging and spectroscopic technique, allowed to follow the evolution of HCCI combustion process. A comparison with CR injection strategy was carried out.

2. Experimental apparatus and engine operating conditions

The transparent diesel engine used is a single cylinder, direct injection, four stroke diesel engine equipped with the head of real engine (1.9l, 16v JTD) to preserve the air intake flow, and with last generation Common Rail injection system. The engine has a bore of 85 mm, a stroke of 92 mm, and a compression ratio of 17.7:1. The design of the engine utilized a classic extended piston with piston crown window (diameter of 34 mm). The piston crown window provided a full view of the combustion bowl locating an appropriate 45° UV-visible mirror inside the extended piston. Moreover, a steel crown was placed between the cylinder head and cylinder block. This allowed the arrangement of three windows to provide orthogonal and longitudinal optical accesses. Finally, a window in the cylinder head was obtained. More details and specifications on engine are reported in ref. [4-5]. The engine was equipped with last generation Common Rail injection system operating at maximum injection pressure of 1800 bar. A fully flexible Electronic Control Unit (ECU) lead it for combustion optimization. In particular, the ECU controlled the number of injections (till 5) per cycle, the start and the duration of injection as well as the dwell time between the consecutive injections. The injector was located centrally and had the same cylinder axis, it was equipped with a single guide microsac nozzle. Imaging and chemiluminescence flame emission analysis from ultraviolet (UV) to visible were performed by means of the experimental set-up shown in figure 1. In particular, to better examine the temporal and spatial evolution of spray and flame, images were acquired through the piston crown window and 45° mirror, placed in the elongated piston, by two different CCD cameras with different capability. The first had high sensibility in the UV range (512x512 pixels with every pixel of 24x24 μm^2), and the second one (640 x 480 pixels with every pixel of 9.9x9.9 μm^2) was sensible in the visible. In order to obtain more detailed information on the species that occurring during the combustion process, emission flame were collected and focused on the entrance slit of a spectrograph through an UV objective (Nikon 78 mm f/3.8). The spectral image formed on the spectrograph exit plane was matched with a gated intensified CCD (ICCD) camera (512x512 pixels). More details and specifications about the optical apparatus are reported in ref. [4-5, 7-8]. Data were detected with the spectrograph placed at central working wavelength of 400 nm and the intensifier-gate duration of 83 μs in order to have a good accuracy in the timing of the onset of the combustion. Chemiluminescence signals, due to radical emission species, were detected in several locations of the combustion chamber with high spatial resolution. Radicals and flame imaging were acquired with the same ICCD and UV and visible narrow band pass filters chosen at characteristic wavelength of OH (λ =309 nm) and HCO (λ=380 nm). Synchronization of engine with ICCD and CCD camera was obtained by the unit delay connected with signal coming from the engine shaft encoder.

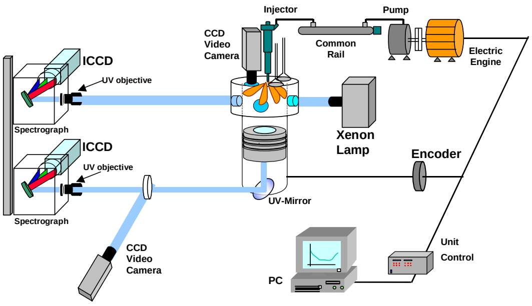

Fig. 1 Experimental apparatus for optical measurements.

All the data presented in this paper was taken at engine speed of 1000 rpm using commercial diesel fuel. When engine operated in diesel standard mode, the intake air temperature and pressure were set to 320 K and 1.33 bar, respectively. At motored condition, temperature and density at Top Death Center (TDC) were estimated, assuming a polytropic coefficient of 1.36 [6]. They are 803 K and 18.9 kg/m^3, respectively. Instead, in HCCI mode intake air temperature and pressure were set to 312 K and 1 bar, respectively. At TDC, temperature and density were 787 K and 14.8 kg/m^3, respectively, assuming the polytropic coefficient of 1.36. This operating condition avoided knocking and misfire phenomena. Diesel standard mode, with three injections per cycle, was compared to HCCI one, Figure 2. During HCCI mode, five short injections were injected during the compression stroke far from the top death center. For CR strategy an injection pressure of 600 bar was used because this value was adapted for this engine displacement, while for HCCI process the pressure was set to 700 bar to keep as low as possible the injection time and in order to inject the same amount of fuel of Pre+Main+Post strategy. In table 1 injection strategies specification are reported.

	P_{inj} [bar]	T_{in} [°C]	P_{in} (abs) [bar]	Fuel [Kg/h]	BMEP [bar]	SOI Pilot [°]	ET Pilot [μs]	SOI Pre [°]	ET Pre [μs]	SOI Main [°]	ET Main [μs]	SOI Post [°]	ET Post [μs]	SOI After [°]	ET After [μs]
Pre+Main+Post	600	44	1.33	0.32	3.0	\	\	-9	400	-4	625	11	340	\	\
HCCI	700	35	1	0.30	2.4	-70	400	-60	400	-50	400	-40	400	-30	400

Table 1 Engine strategies specifications.

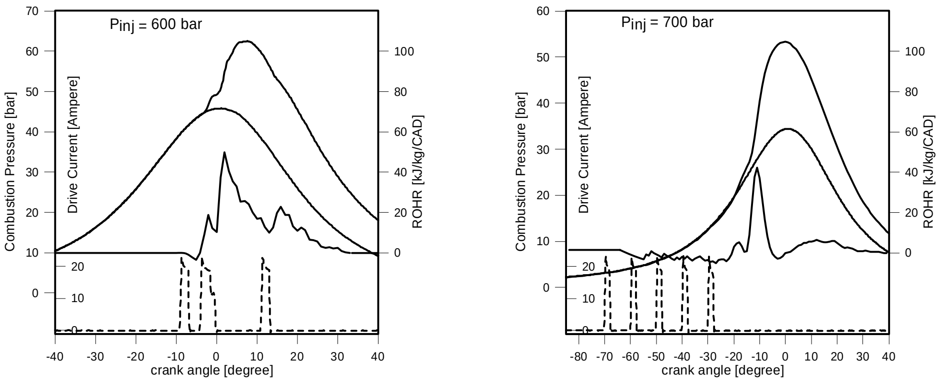

Fig. 2 Histories of cylinder pressure, rate of heat release and drive current versus crank angle at 1000 rpm for CR (left) and HCCI (right) injection strategies.

3. Results and discussion

To investigate the autoignition and early soot formation of homogeneous combustion, chemiluminescence and natural flame emissions measurements has been carried out. The characterization has allowed to elucidate the physical and chemical process involved. Autoignition is commonly defined as the crank angle where the apparent heat release shows a minimum. This point indicates that the energy release, due to combustion exothermic reactions, begins to exceed the energy losses due to the fuel evaporating process [6]. Because chemiluminescence is produced directly by the exothermic chemical reactions, it marks the location of the initial combustion reactions with high temporal and spatial resolution. By the analysis of the combustion cycle for HCCI of figure 2, the autoignition is observed at 23° btdc. It is due to the low temperature reactions [2, 3] and it has a duration of 1.3 ms. At the end of this phase (15° btdc), the rate of heat release curve decreases and fastly increases due to the high temperature reactions, and a change in slope of the combustion pressure curve is observed.

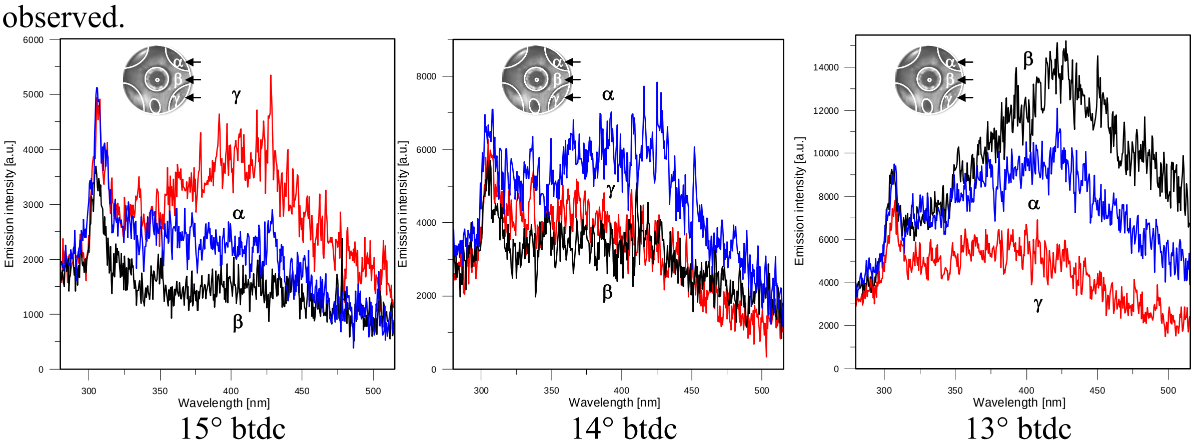

Fig. 3 Chemiluminescence emission spectra @ 1000 rpm engine speed and Pinj = 700 bar.

In figure 3 are showed the spectra detected from the start of high temperature reactions until 13° btdc. Spectral chemiluminescence measurements showed a weak flame emission, in the near ultraviolet range. The spectra are acquired in the location under the intake valves where the highest chemical activities are observed. At 15° btdc, spectra from different location have similar behaviour and intensity. The broadband emission centered at 380 nm is associated to the presence of HCO. The appearance of this radical is recognized by other authors [9-10]. Then, the presence of OH and CH radicals with their characteristic peaks at 309 nm and 431 nm, respectively, are well resolvable [4, 7, 8-10]. OH is a marker of fuel oxidation and premixed combustion, and appears in the location with high local air-fuel ratio. On the other hand, CH is detected near the wall where fuel impinged and is characteristic of rich mixture combustion. At 14° btdc, all the spectra increase their intensities and the spectral features change for all the locations investigated. OH radical has similar intensity in all the chamber due to continuous evolution of premixed combustion. At 13° btdc, the flame intensities are higher than previous crank angles, and OH radical is still the dominant species. At increasing crank angles, a continuum spectrum in the range 350 – 450 nm is revealed everywhere in the chamber. This is characteristic of the CO continuum indicating the flame temperature increases. The CO continuum spectrum maybe superimposed on the spectrum of the HCO emission band [10-11].

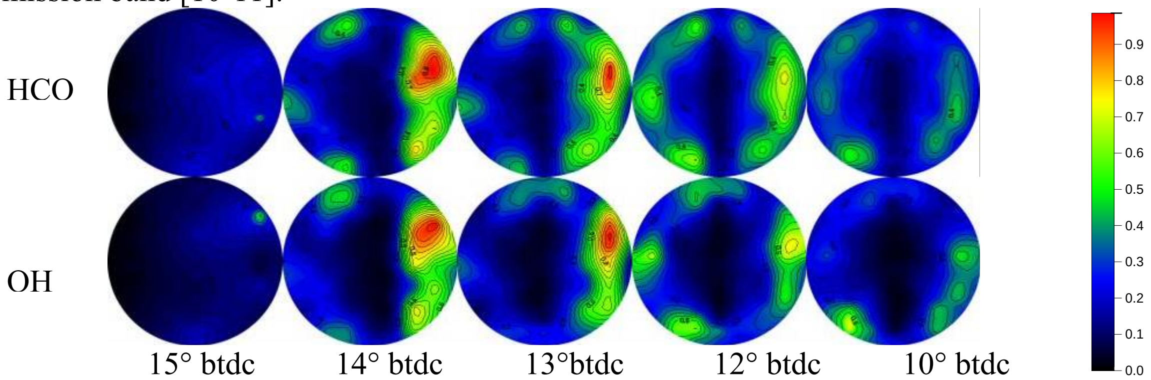

Fig. 4 Normalized HCO and OH spatial distributions and temporal evolutions @ 1000 rpm engine speed and Pinj = 700 bar.

Figure 4 reports the location of autoignition in terms of HCO and OH radicals. Spatial distribution and temporal evolution were detected in the bowl with ad-hoc filters. Due to the high ignition delay, around 1.8 ms, the mixture in the chamber results well homogenised and the chemiluminescence activity seems to be well distributed on the right side. Figure 43 shows that the first detectable contribute of HCO radical occurs at 15° btdc. Before 15° btdc the emission signal detected are not resolvable. As observed in other papers, during the autoignition phase the majority of the chemiluminescence is detected in the region with high amount of fuel vapour phase [7, 13].Then after a crank angle, at 14° btdc, HCO reaches its maximum value in the bowl, and starts to distribute homogeneously all around the outer radius of the combustion chamber. The maximum of HCO signal occurs slightly before the peak of rate of heat release (Fig. 2). At 13° btdc, chemiluminescence activity propagates toward the centre filling the bowl. Then, HCO intensity decreases and disappears at 8° btdc. On the other hand, the OH radical starts at same crank angle of HCO, increases rapidly, and reaches the maximum intensity in 1° crank angle. Then the OH is reduced by the soot flame propagation, and, around the top death centre, decreases completely when the premixed combustion cesses. The decrease of OH radical is slower than HCO one.

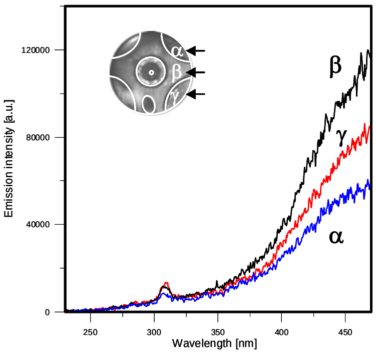

Fig. 5 Chemiluminescence emission spectra @ 1000 rpm engine speed and Pinj = 700 bar at 8° btdc.

Figure 5 reports UV-visible emission spectra measured at 8° btdc. A broad band emission in the visible region is resolvable. This spectral feature is similar to Planck black body emission curve and indicates the first soot formation. The first soot signal is observed around 21° crank angles (around 3.5 ms) after the end of last injection. This time corresponds with the start of soot formation. Different slopes are related to different soot amount in the chamber.

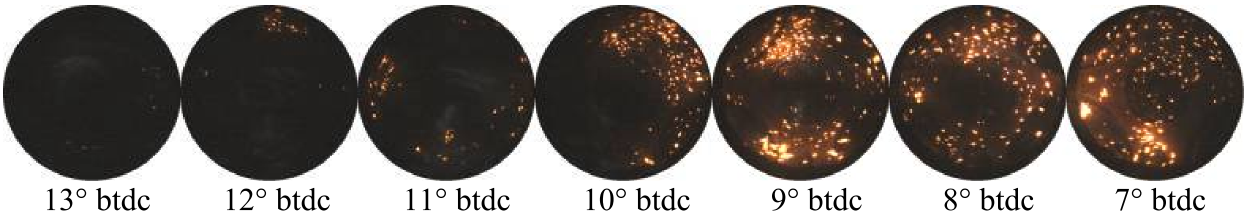

Fig. 6 Digital imaging of visible combustion acquired with CCD camera @ 1000 rpm engine speed and Pinj = 700 bar.

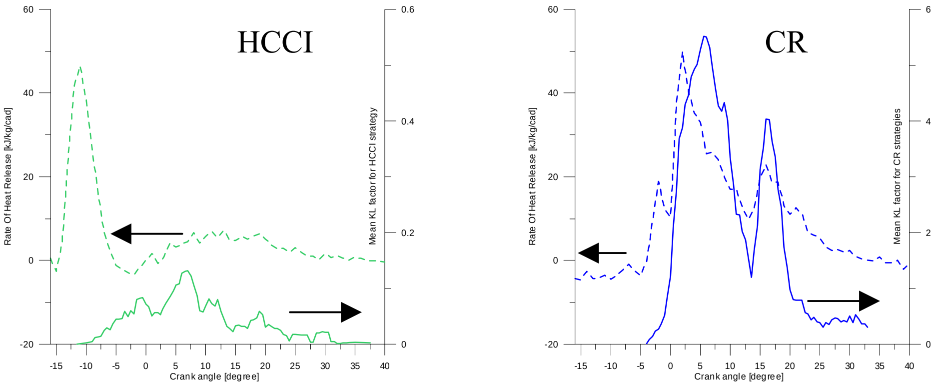

Fig. 7 Mean KL factor and rate of heat release versus crank angle for HCCI (left) and CR (right) injection strategies.

At 13° btdc the first visible flame is observed using a detector with high spatial resolution (fig. 6). Small spots are visible and their intensity grow up in all the chamber increasing crank angles. Even if, the dimensions seem do not change during all the combustion process. These little spots are distributed homogeneously. At 12° btdc the first bright spots are probably due to small pockets of fuel that were spread in the mixture. Then the autoignition proceed and the soot formation occurs. Figure 7 reports the soot amount (KL factor) versus crank angle for both conventional CR diesel mode and HCCI one. The HCCI soot amount is smaller compared with standard diesel one, already in the combustion chamber (Fig. 8). The rate of heat release for HCCI mode shows a well resolvable peak characteristic of combustion that develops in premixed mode and its duration is considerably short with respect to Pre+Main+Post strategy. On the other hand, the CR rate of heat release shows diffusive combustion responsible of soot formation. It can be noted that the wide presence of OH radicals, until 8° btdc, contribute to inhibit the soot formation with respect to CR diesel mode.

4. Conclusion

In the present paper optical diagnostics were applied to a transparent CR DI diesel engine operating in conventional diesel mode and HCCI one.

UV and visible digital imaging and chemiluminescence spectroscopy were carried out in order to investigate autoignition and combustion.

The first detected stages of HCCI combustion were due to UV luminous flame around 8.8 ms from the start of the first injection. The combustion started under the intake valves and then developed from the outer radius of the chamber toward the centre. In particular, HCCI mode

ignited as an homogeneous lean charge over the entire combustion chamber showing spots luminous combustion.
In order to evaluate the reactions that occurred in the chamber from start of autoignition to combustion HCO and OH radicals are detected. They were homogenously distributed in the chamber. Increasing the time, HCO disappeared while OH radical remained widely spread in the chamber during the whole combustion process. The start of soot formation occurred after 3.5 ms the end of the last injection. In several locations of small size the soot was present in low concentrations. The wide presence and high OH concentration seemed to inhibit the formation of soot. This promoted OH as a marker of HCCI mode combustion. Moreover, being the control of the ignition timing a central objective for optimise the HCCI engine operation, HCO and OH could be a suitable tools to identify the start of combustion and phase the rate of heat release.

Acknowledgments

The authors would like to thank Mr. Carlo Rossi and Mr. Bruno Sgammato for their precious help and technical support.

References

1) Assanis, D. N., Najt, P. M., Dec J. E., Eng J. A., Asmus T. N., Zhao F., “Homogeneous Charge Compression Ignition (HCCI) Engines”. Key research and Development Issues. SAE International 2003.
2) Denbratt, I., Helmantel, A: “HCCI Operation of a Passenger Car Common Rail DI Diesel Engine With Early Injection of Conventional Diesel Fuel”. SAE Paper 2004-01-0935, 2004.
3) Ryan, T.W. and Callahan T.J., “Homogeneous Charge Compression Ignition of Diesel Fuel”, SAE Paper 961160, 1996.
4) Corcione, F.E., Di Iorio, S., Mancaruso, E., Merola, S.S., Vaglieco, B.M., “Combustion Diagnostics of a Diesel Engine with Multiple Injection”. THIESEL 2004 Conference on Thermo and Fluid Dynamic Processes in Diesel Engines, pp 297-308, 2004.
5) Merola, S.S., Vaglieco, B.M., Corcione, F.E., Mancaruso, E., “In-cylinder Combustion Analysis by Flame Emission Spectroscopy of Transparent CR Diesel Engine”. SAE Paper n° 2003-01-1112, 2003.
6) Heywood, J. B., “Internal Combustion Engine Fundamentals” - Mc Graw-Hill, NewYork, 1988.
7) Merola, S.S., Vaglieco, B.M., Corcione, F.E., Formisano, G., “Spectral Analysis of Combustion Process of Common Rail Diesel Engine”. SAE Paper n° 2002-01-1634, 2002.
8) Astarita, M., Corcione, F. E., Vaglieco, B. M., Valentino, G., “Optical Diagnostics of Temporal and Spatial Evolution of a Reacting Diesel Fuel Jet”. Combustion Science and Technology, vol. 48, 1-16, 1999.
9) Gaydon, A. G., “The spectroscopy of flames”. Chapman and Hall, London, 1974.
10) Murase, E., Hanada, K., Miyaura, T., Ikeda, J., Konishi, N., “Experimental Studies of HCCI Combustion”. COMODIA 2004, 2004.
11) Sheinson, R. S., Williams, F. W., Combustion and Flame, 21, pp. 221-230, 1973.
12) Espey, C., Dec, J. E., Litzinger, T. A., Santavicca, D. A., “Planar Laser Rayleigh Scattering for Quantitative Vapor Fuel Imaging in a Diesel Jet”, Combustion and Flame, Vol. 109, pp65-86, 1997.